Macromolecules

ARTICLE

pubs.acs.org/Macromolecules

Shape Memory Behavior of Zinc Oleate-Filled Elastomeric Ionomers

Jing Dong and R. A. Weiss*

Department of Polymer Engineering, University of Akron, Akron, Ohio 44325, United States

ABSTRACT: Shape memory elastomeric compounds were prepared from mixtures of the zinc salt of a sulfonated poly{ethylene-*r*-propylene-*r*-(5-ethylidene-2-norbornene)} ionomer (Zn-SEPDM) and zinc oleate (ZnOl). Physical cross-links in the ionomer due to interchain ionic interactions provided a "permanent" cross-linked network, and strong dipolar interactions between the ionomer and a dispersed phase of crystalline ZnOl provided a temporary network. ZnOl concentrations as high as 50 wt % were studied. A temporary shape was achieved and fixed by deforming the compound above the melting point (T_m) of the ZnOl (~78 °C) and then cooling the material under stress to below T_m. The permanent shape was recovered by reheating the sample to above T_m without an applied stress. The materials were characterized by thermal analysis, X-ray diffraction, dynamic mechanical analysis (DMA), and tensile tests, and the shape memory behavior was measured by DMA and static stretching experiments. Although shape fixing efficiencies of up to 90% were achieved, significant creep recovery of the temporary shape occurred over a time period of ~300 h, which was attributed to reorganization of one or both of the physical networks. The materials exhibited high shape recovery efficiencies, but that, too, was affected by viscous effects associated with the retention of the temporary shape.

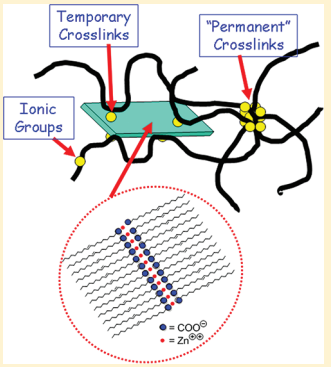

INTRODUCTION

Shape memory polymers (SMP) are materials that can change shape when exposed to an external stimulus, such as temperature, light, moisture, or electricity.[1] Thermally activated SMPs have a permanent shape that is provided by a cross-linked network. They can be deformed above a specific actuation temperature (T_{act}) of a second, reversible network and fixed into a temporary shape when cooled under stress to below T_{act}. The temporary shape is stable until the sample is reheated to above T_{act} in the absence of an external stress, and then the material reverts to its permanent shape. SMPs have applications as medical devices (e.g., stents and sutures), actuators, sensors, artificial muscles, switches, smart textiles, and self-deployable structures. A number of recent reviews have surveyed the materials and applications for SMPs.[1−6]

The cross-linked network used for the permanent shape may be a covalent network or a physical network with sufficiently long relaxation times that the polymer behaves as a cross-linked polymer during the time frame of the application.[2] For thermally activated SMPs, the temporary network is a thermally reversible, physical network that is usually formed by a glassy polymer phase, a crystalline polymer phase, strong intermolecular interactions such as hydrogen bonding, ionic, or charge-transfer interactions, or nanophase separation such as occurs in block copolymers.

Liu et al.[2] classified thermally activated SMPs into four main types based on the mechanism of the transition temperatures: (1) covalently cross-linked glassy polymers where the glass transition temperature was the actuation temperature (i.e., $T_g = T_{act}$); (2) covalently cross-linked, semicrystalline elastomers where T_{act} is the melting temperature of the polymer ($T_m = T_{act}$); (3) physically cross-linked, glassy thermoplastics where $T_g = T_{act}$; and (4) physically cross-linked, semicrystalline block copolymers where the melting point of a soft segment nanophase is T_{act}. Note that the shape memory behavior of nearly all reported SMPs depends entirely on the thermal transitions of a polymer or mixtures of polymers. Variation of the modulus and actuation temperature of the material may be achieved by incorporating fillers, though both cannot be changed independently, and oils and other inert fillers may be added to lower the cost of the material. The actuation temperatures for most shape memory polymers, however, depend on a physical or thermodynamic property of the polymer(s). As a result, with few exceptions,[7] any desired changes of T_{act} and/or modulus usually require the development of a new composition or polymer.[1−9]

We recently reported a new concept for a shape memory polymer that consisted of a low molecular weight fatty acid or fatty acid salt (FAS) compounded with an elastomeric ionomer, the zinc salt of sulfonated poly{ethylene-*r*-propylene-*r*-(5-ethylidene-2-norbornene)}, Zn-SEPDM.[8] In that case, the physical cross-links in the ionomer due to the nanophase separation of the ionic species provided a permanent shape, while the strong intermolecular interactions between FAS and Zn-SEPDM formed a thermally reversible, physical network that provided the temporary cross-links needed for the SMP. The key advantage and versatility of such an approach is that the T_{act} of an SMP can be varied over a wide range of temperatures, e.g., from 20 to 120 °C, simply by choosing an appropriate fatty acid or salt, while using the same host elastomer.[10]

The surprising aspect of those SMPs was that the dipolar interactions between the ionomer and the FAS were sufficiently

Received: August 23, 2011
Revised: October 9, 2011
Published: October 27, 2011

strong so that the dispersed particles of the FAS were able to support stress. The compounds exhibited excellent shape fixing and shape recovery, but in the experiments reported in ref 8, little time elapsed between the shape fixing and shape recovery steps. The question that motivated the research reported herein was how robust were the physical cross-links used to develop the temporary and permanent networks in the FAS/ionomer compounds. That question and a more detailed description of the compounds are addressed in this paper for compounds prepared from zinc oleate (ZnOl) and Zn-SEPDM.

EXPERIMENTAL SECTION

Materials. Royalene 521, a poly{ethylene-*r*-propylene-*r*-(5-ethylidene-2-norbornene}, EPDM, containing 52 wt % ethylene, 48 wt % propylene, and 4.7% ethyldiene−norbornene and having a Mooney viscosity of 45 at 100 °C was obtained from Crompton Chemical Co. ZnOl (99% purity) was purchased from Shepherd Chemical Co. Both were used as received.

Zn-SEPDM was prepared by sulfonating EPDM with acetyl sulfate and neutralizing the product with zinc acetate.[8,9] The sulfonation level of the Zn-SEPDM used in this study was 16.6 mequiv per 100 g of rubber (mequiv phr) as determined by elemental sulfur analysis.

Zn-SEPDM/ZnOl compounds ranging in composition from 0−50 wt % ZnOl were prepared by codissolution in a 95/5 (v/v) mixture of toluene and methanol. The compounds were recovered by evaporating the solvent, washing first in boiling distilled, deionized water, and then with methanol in a Waring blender. The compounds were subsequently vacuum-dried overnight at 50 °C. Films of the Zn-SEPDM/ZnOl compounds were prepared by compression molding at 150 °C. In this paper, the sample notation used for the Zn-SEPEM/ZnOl compounds is Zn-SEPDM(x), where x represents the wt % ZnOl. It is significant to note that even with a concentration of 50 wt % ZnOl, the compounds were relatively clear or translucent, which is in stark contrast to the addition of ZnOl to unsulfonated EPDM. In that case, less than 1 wt % ZnOl turns the compound white and opaque, and the waxy ZnOl blooms to the surface. As was discussed in ref 10 for zinc stearate added to Zn-SEPDM, the very strong interaction between a FAS and the ionomer leads to high compatibility of these mixtures.

Materials Characterization. The melting transition temperature of ZnOl was with a TA Instruments DSC Q100 using aluminum sample pans, a nitrogen atmosphere, and cooling and heating rates of 10 °C/min. The melting temperature of the ZnOl was defined as the peak temperature of the melting endotherm. The thermal stability of the compounds was measured using a TA Instruments TGA 2950 thermogravimetric analyzer (TGA) from room temperature to 600 °C with a heating rate of 10 °C/min and a dry N_2 atmosphere.

A TA Instruments DMA 2980 dynamic mechanical analyzer (DMA) with a tensile film fixture was used to measure the glass transition temperature, T_g, and the temperature dependence of the complex tensile modulus. The dynamic mechanical properties of rectangular films (15 × 5 × 1 mm) were measured using a multistrain measuring mode, a frequency of 1 Hz, a preload force of 0.005 N, and a temperature ramp from −100 to 200 °C at 5 °C/min. T_{act} was also measured during these temperature scans. The tensile stress−strain behavior of the compounds was measured with an Instron model 1101 universal testing machine using a 44.5 N load cell. Film samples were cut into dog-bone specimens with gauge length dimensions of ∼8.8 × 3.3 × 0.6 mm. The tests were carried out at room temperature (∼23 °C) using a crosshead speed of 5 mm/min.

Wide-angle X-ray diffraction (WAXD) of the neat components and compounds was measured with a Bruker D8 Discover X-ray diffractometer with a general area detector diffraction system (GADDS) using chromium radiation (λ = 0.2291 nm) and an exposure time of ∼20 min. The real-space distance, d, corresponding to the diffraction data was calculated from Bragg's law, $d = 2\pi/q$, where the scattering vector $q = 4\pi \sin(\theta)/\lambda$ and θ is one-half the scattering angle.

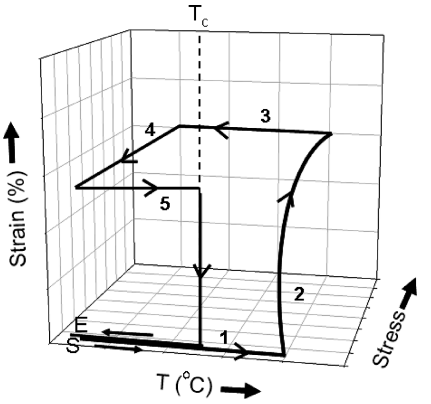

Figure 1. Ideal shape memory cycle. S denotes the start of the cycle. The sample is heated without an applied stress along path 1. Above T_c (denoted by the dotted line), stress is applied (path 2) to stretch the sample. The deformed sample is then cooled under stress along path 3, and the stress is removed along path 4 to set the temporary deformed shape. When the sample is reheated (path 5), it recovers its permanent shape. The sample can then be cooled to end the cycle (E). If the recovery is 100%, S and E denote the same point of the graph.

Shape Fixing Experiments. Shape fixing refers to how well the sample holds the temporary shape with time. Three rectangular samples with dimensions ∼3 × 30 × 0.5 mm were cut from ∼0.5 mm thick films for each composition. The samples were immersed into boiling water (100 °C), stretched to 33−63% strain, and then quenched in an ice bath (0 °C) while still under stress to fix the temporary shape. The samples were then stored at ambient conditions without stress, and their length was measured every 10 min for the first hour, then every subsequent hour for 8 h, and then daily for 21 days to determine how well the fixing held. The shape fixing effectiveness, $F(t)$, is defined by eq 1[10]

$$F(t) = \frac{L_f(t)}{L_s} \times 100\% \quad (1)$$

where L_s is the original stretched length and $L_f(t)$ is the length of the sample at time, t, after the stretching step.

Shape Recovery Experiments. Shape recovery refers to how well the sample recovers to its original shape when it is heated to above T_{act}, i.e., when the sample reverts from the temporary shape back to the permanent shape. Two different shape recovery experiments were run. In the first case, the samples used in the time-dependent shape fixing experiments described in the previous section were reheated in boiling water after they had been allowed to relax for 21 days at room temperature. The shape recovery, R, is defined by eq 2[12]

$$R = \frac{L_s - L_r}{L_s - L_i} \times 100\% \quad (2)$$

where L_s is the stretched length and L_r and L_i are the length after recovery and the length of the original sample before the shape memory experiment was performed. In the second experiments, fresh rectangular samples were immersed in boiling water, stretched 33−63%, and then quenched in ice water to fix the temporary shape. In this case, the sample was immediately reheated to recover the original shape, without allowing the sample time to relax. The shape recovery was also calculated from eq 2.

Shape Memory Cycle. The shape memory properties, shape fixation and shape recovery, were also measured using the DMA with a tensile film fixture. A schematic of an ideal shape memory cycle is shown in Figure 1 and described in the figure caption. For the

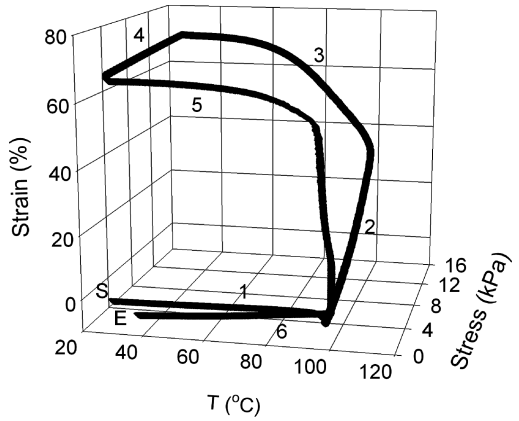

Figure 2. Shape memory cycle for Zn-SEPDM(10). S denotes the start of the cycle. The sample was heated without an applied stress along path 1 to 99 °C, at which point it was stretched ~36%, path 2. The stress was removed along path 4 to set the temporary deformed shape. The sample was reheated (path 5), and shape recovery began at ~70 °C (T_c). Heating was continued until the temperature reached 100 °C. The sample was held at 100 °C for 30 min and then cooled to end the cycle (E).

Zn-SEPDM SMPs, a shape memory cycles was carried out by first heating the sample to 100 °C from ambient temperature (~23 °C) with a preload force of 0.005 N. After the sample equilibrated at 100 °C, the force was increased to 0.050 N to stretch the sample, and then the sample was cooled quickly to 50 °C to fix the temporary shape. The force was lowered to 0.005 N, which was sufficient to maintain tension on the film. The sample was then reheated at 2 °C/min to 100 °C and held at constant force for 30 min to allow for any strain recovery. It is important to note that for these cycles the time that the sample is held between the paths shown in Figure 1 is short, which minimizes any observation on nonideality of the shape memory behavior—specifically viscoelastic behavior.

■ RESULTS AND DISCUSSION

An example of a shape-memory cycle for Zn-SEPDM(10) is shown in Figure 2. In this case, the strain increased substantially as the sample was cooled under load from ~100 to 30 °C (path 3 in Figure 2). That result was surprising, since cooling the sample leads to the crystallization of ZnOl, which increases the modulus of the compound. So, if anything, one would expect at constant stress the strain to decrease during this step. The elongation may indicate some creep of the "permanent network", which is a consequence of the physical nature of the permanent network in these materials, i.e., the dipolar cross-links due to microphase-separated ionic domains.[11] An alternative explanation is that the elongation of the network occurs as a consequence of anisotropic crystallization of the fatty acid with a preferred orientation in the stretching direction. That explanation has been used to explain the lengthening of semicrystalline polymers[12,13] when cooled under a tensile deformation. Preliminary X-ray characterization of uniaxially deformed zinc steatate (ZnSt)/Zn-SEPDM SMPs indicates that the ZnSt lamellae orient in the stretching direction, which suggests that the latter explanation may also be valid for the SMPs described in this paper. However, additional X-ray studies during deformation and crystallization of the ZnOl are needed to definitively confirm the source of the sample elongation during the cooling step shown in path 3 of Figure 2.

The sample did, however, hold its shape once the zinc oleate crystallized to form the temporary network. After removing the external stress (path 4 in Figure 2), the sample was held at 30 °C for about 30 min, during which time very little change in the strain occurred.

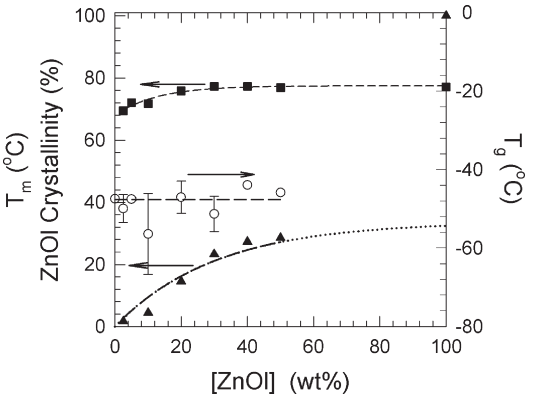

Figure 3. (○) T_g of Zn-SEPDM (DMA), (■) T_m of ZnOl (DSC), and (▲) relative crystallinity of ZnOl (DSC) in Zn-SEPDM/ZnOl compounds as a function of ZnOl concentration.

When the sample was reheated at 2 °C/min, the original shape began to recover at ~70 °C (path 5 in Figure 2), though the major shape recovery occurred between 90 and 100 °C. That is a consequence of the relatively broad melting transition of the ZnOl in the compound. The sample was held, without stress, at 100 °C for 30 min to allow the recovery process to reach equilibrium. When the sample was then cooled to room temperature, the length retracted beyond the original length, to ~4% shorter, which actually corresponds to ~104% shape recovery. A recovered length shorter than the original length was surprising in view of the apparent creep of the network during the cooling part of the shape fixing step (step 3 in Figure 2). One explanation for this may be residual stresses the resulted from the processing the film samples. Thus, although these materials exhibited shape memory, there were aspects of the shape memory process that were not consistent with the formation of elastic networks, and the remainder of this paper is directed at developing an understanding of the viscoelastic nature of the two physical cross-links responsible for shape memory in these ionomer compounds.

Characterization of the Zn-SEPDM/ZnOl Compounds. The thermal transitions of the Zn-SEPDM/ZnOl compounds as a function of ZnOl content are shown in Figure 3. The T_g of the Zn-SEPDM, measured by DMA, remained relatively constant with the addition of ZnOl, but the T_m of the ZnOl in the compounds, measured by DSC, decreased with decreasing ZnOl concentration. The relative crystallinity of ZnOl in the compounds was estimated from the ratio of $\Delta H/\Delta H_{ZnOl}$, where ΔH was the measured value for the ZnOl in the compound and ΔH_{ZnOl} was the corresponding experimental value for the neat ZnOl. The relative crystallinity of the neat ZnOl was arbitrarily set to 100% for comparison. ZnOl crystallization was suppressed by the presence of the Zn-SEPDM. The melting point depression and the large reduction in the ZnOl crystallization are a consequence of the strong intermolecular interactions between the ZnOl and the ionomer. That interaction promoted a very fine dispersion of small ZnOl particles and, perhaps, even miscibility of the amorphous ZnOl. Miscibility would not be surprising in light of the findings by Wakabayashi and Register that magnesium stearate is miscible with polyethylene-based ionomers in the melt.[14]

The thermal degradation behavior of the Zn-SEPDM, ZnOl, and the compounds with 20 and 50 wt % ZnOl is shown in Figure 4.

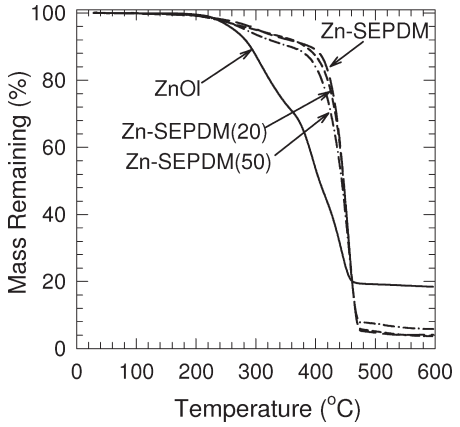

Figure 4. Thermogravimetric analysis of ZnOl, Zn-SEPDM, Zn-SEPDM(20), and Zn-SEPDM(50). Experiments were run using a nitrogen atmosphere.

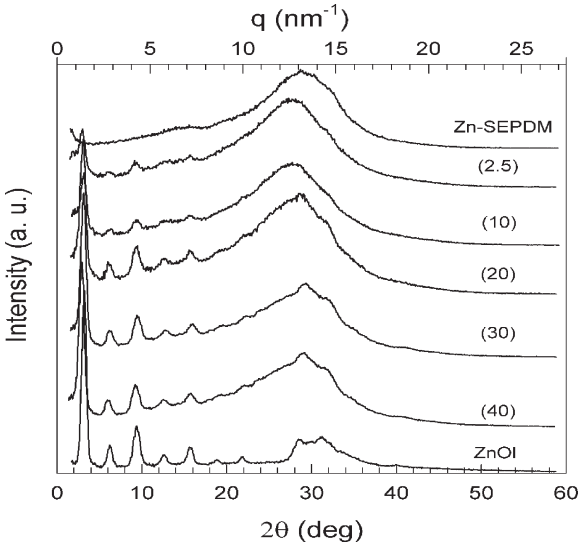

Figure 5. Wide-angle X-ray diffraction of compression-molded films of Zn-SEPDM, the ZnOl/Zn-SEPDM compounds, and the neat ZnOl powder.

A small mass loss from Zn-SEPDM and its compounds with ZnOl above 100 °C was due to absorbed water. Decarboxylation of the ZnOl occurred above 250 °C, and that process was followed by degradation of the hydrocarbon chain above ~350 °C.[15,16] Otherwise, the ionomer and the compounds were relatively stable to 200 °C. The mass loss for the ionomer and compounds between ~250 and 375 °C is due to a combination of decarboxylation of the ZnOl and desulfonation of the ionomer. Pyrolysis of the hydrocarbon chain occurred above ~375 °C. The char residue in ZnOl, Zn-SEPDM, and the compounds is due to zinc and or the formation of zinc oxides. The key conclusion from the TGA data is that the degradation of the shape memory compounds was not a factor in the experiments described herein, since the temperature was always kept below 150 °C.

Wide-angle X-ray diffraction data for the ZnOl/Zn-SEPDM compounds and the neat components are shown in Figure 5. The Zn-SEPDM was amorphous. The neat ZnOl was a crystalline powder with a high degree of order. Ten distinct peaks were resolved in the neat ZnOl diffraction pattern (see Figure 6) with

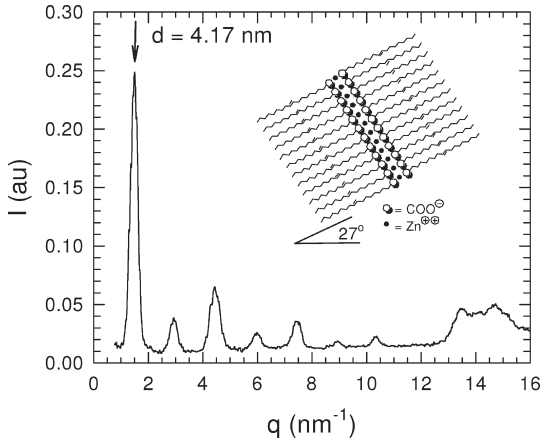

Figure 6. X-ray diffraction of ZnOl. A fully extended structure of ZnOl is also shown. The numbers above the arrows identifying the diffraction peaks correspond to the *d*-spacings calculated by Bragg's law.

the positions of the maxima very close to a ratio of q_n/q_1 = 1:2:3:4:5:6:7:8:9:10, where q_1 is the first reflection in the X-ray pattern (i.e., the long-spacing) and n is the subsequent reflection numbers (2−10). That scattering pattern represents a lamellar structure with a periodicity of d. In this case, d = 4.17 nm for a ZnOl, which is consistent with the 4.18 nm reported by Barman and Vasudevan,[17] who concluded that the structure was a tilted bilayer structure with a tilt angle of 27° (see Figure 6).

DMA results for the parent EPDM, the Zn-SEPDM ionomer, and two Zn-SEPDM/ZnOl compounds are shown in Figure 7. The un-cross-linked EPDM had a T_g of about −47 °C and began to flow almost immediately following the transition region. Although the T_gs of the EPDM and the Zn-SEPDM ionomer were about the same, the ionomer was an elastic rubber with a modulus $E' \sim 4$ MPa at temperatures above the transition region, while EPDM was a viscous liquid. The elastomeric nature of the ionomer persisted to above 175 °C, where E' was still ~1 MPa. The T_g of the compounds was relatively insensitive to the addition of ZnOl. Above T_g and below T_m of the ZnOl, the modulus of the SMP increased with increasing ZnOl concentration, but above T_m the modulus decreased with increasing ZnOl (see Figure 8).

The rubber-like nature of the neat Zn-SEPDM above T_g was due to the intermolecular dipole−dipole interactions that occur between the metal sulfonate groups, which produce a physical cross-linked network of microphase-separated, ion-rich nanodomains. The higher modulus for the Zn-SEPDM/ZnOl compounds below the T_m of the ZnOl is a consequence of reinforcement of the ionomer by the ZnOl crystals and the formation of a second network from strong interactions between the metal carboxylate groups of the ZnOl and the metal sulfonate groups of the ionomer.

A number of relationships have been developed for the modulus of particle-filled elastomers, including a semiempirical model by Sato and Furukawa[18] that includes a term to account for the adhesion efficiency between the filler and the polymer, eq 3

$$\frac{E_c}{E_m} = \left[1 + \frac{1}{2}\frac{x^2}{1-x}\right]\left[1 - \frac{\lambda x^3}{3}\left(\frac{1 + x - x^2}{1 - x + x^2}\right)\right] - \left[\frac{\lambda x^2}{3(1-x)}\left(\frac{1 + x - x^2}{1 - x + x^2}\right)\right] \quad (3)$$

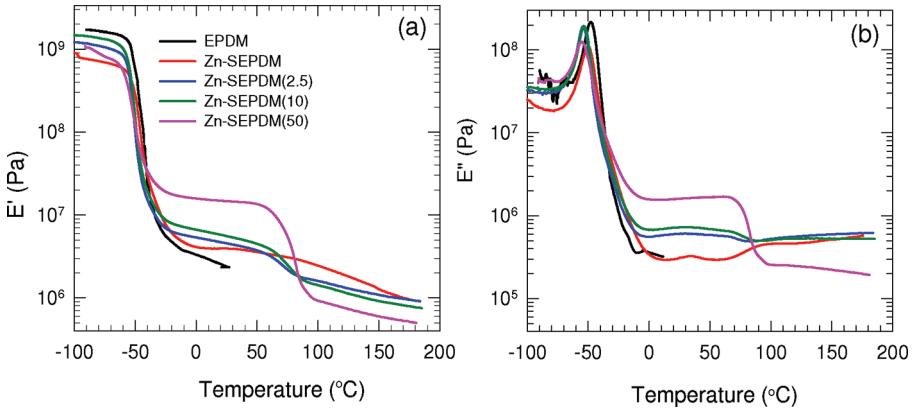

Figure 7. (a) Dynamic storage tensile modulus and (b) loss modulus as a function of temperature for EPDM, Zn-SEPDM, and compounds containing 2.5, 10, and 50 wt % ZnOl.

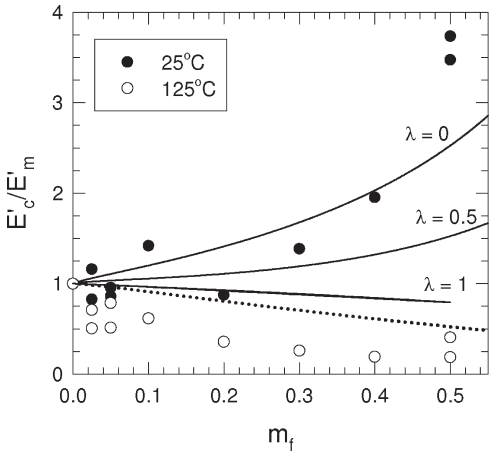

Figure 8. Relative dynamic tensile modulus of Zn-SEPDM/ZnOl compounds at 25 and 125 °C as a function of ZnOl mass fraction. E_c is the dynamic tensile modulus of the compound, and E_m is the modulus of the neat SEPDM. The solid lines correspond to fits of eq 3 to the 25 °C data (λ is discussed in the text), and the dotted line is the rubber elasticity prediction, eq 4, for a swollen rubber. It was assumed that the volume fraction of ZnOl was the same as the mass fraction (see explanation in the text).

where E_c and E_m are the moduli for the composite and polymer matrix, respectively, v_f is the volume fraction of filler, $x = v_f^{1/3}$, and λ is an adhesion factor, which is zero for perfect adhesion and one for no adhesion. The solid circles in Figure 8 are the dynamic modulus, E', data at 25 °C for the SMP compounds normalized by the dynamic modulus of the neat ionomer, also at 25 °C. The solid lines are the predictions of eq 3 for λ = 0, 1/2, and 1. Although there is considerable scatter in the data, they are more consistent with a system with very good adhesion between phases. Some of the scatter in the data may be a consequence of the assumption made that the specific gravity of both components, ionomer and ZnOl, were the same, ~1.0. Without knowing the amorphous and crystalline densities of the ZnOl and the effect of sulfonation on the density of EPDM, that assumption, which equates the volume fraction of ZnOl with the mass fraction of ZnOl, is thought to be a reasonable one, but errors would lead to a shift of the data along the volume fraction axis. In any event, a conclusion here of good adhesion between the components is consistent with that made previously that fatty acids and fatty acid salts complex with the metal sulfonate groups of Zn-SEPDM.[10,13]

The open circles in Figure 8 are the normalized dynamic modulus data at 125 °C, which is above T_m of the ZnOl. The large decrease in the modulus of the compounds above T_m and the decrease with increasing ZnOl concentration are a consequence of the disappearance of the hard ZnOl crystalline domains. Melting of the ZnOl domains destroys the temporary network, since the liquid ZnOl cannot support stress. Jackson et al.[13] previously showed that ionic aggregation in the Zn-SEPDM phase of Zn-SEPDM/zinc stearate (ZnSt) compounds persisted to >200 °C. SAXS experiments similar to those used by Jackson et al.[13] were not repeated for the ZnOl compounds, but the DMA data in Figures 7a and 8 are consistent with the conclusion that in this study, as well, the microphase separation of the ionomer, i.e., the permanent network in these SMPs, also remained intact above the T_m of the ZnOl.

Persistence of the permanent network due to the microphase-separated ionic aggregates of the ionomer above T_m was responsible for the rubber-like modulus, ~1 MPa, at relatively high temperatures (see Figure 7a). The reversal of the modulus dependence on ZnOl concentration above T_m, i.e., the modulus decrease with increasing ZnOl concentration, is a consequence, at least in part, of plasticization of the ionomer by the molten fatty acid salt. Similar behavior was previously reported for compounds of Zn-SEPDM containing ZnSt.[11,19] If the effect of the molten ZnOl on the ionomer was simply due to plasticization, however, one would expect that the modulus would follow the prediction of the theory of rubber elasticity, eq 4

$$E = v_f^{1/3} E_0 \tag{4}$$

where E_0 is the modulus of the unswollen rubber network, i.e., the neat Zn-SEPDM. The prediction of eq 4 is given by the dotted curve in Figure 8, and it is clear that the actual moduli of the compounds were considerably less than the rubber elasticity prediction. This disparity is believed to be a due to some solvation of the dipole−dipole associations of the metal sulfonate groups by the molten ZnOl that changes the "permanent" network, which in the SMPs described herein is also derived from physical cross-links. As a result, the molten ZnOl not only plasticizes the ionomer but it also lowers the effective cross-link density of the "permanent" network, which would be expected to detrimentally influence the shape memory behavior.

Tensile stress vs strain curves (engineering stress and strain) for the ZnOl/Zn-SEPDM compounds are shown in Figure 9.

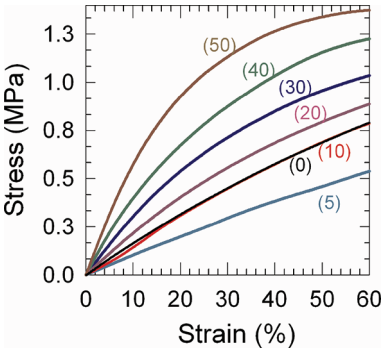

Figure 9. Example engineering tensile stress vs strain for ZnOl/Zn-SEPDM compounds for the first 60% strain. The numbers in parentheses denote the ZnOl concentration (wt %).

Table 1. Tensile Properties of Zn-SEPDM and Zn-SEPDM/ZnOl Compounds

[ZnOl] (wt %)	E_{10} (MPa)	ε_y (%)	σ_y (MPa)
0	1.5		
5	1.1	250	1.2
10	1.4	240	1.3
20	2.1	230	1.3
30	3.1	120	1.2
40	4.0	150	1.5
50	5.7	75	1.4

The modulus (initial slope of the stress−strain curve) decreased when the concentration of ZnOl was 5% but then increased monotonically with increasing ZnOl (see Table 1). The decrease of modulus with 5% addition of ZnOl could be a consequence of the limited solubility of the fatty acid in the ionomer, which plasticizes the ionomer. That is evident from the relatively low value of the ZnOl crystallinity in the compound (see Figure 3). Above 5% ZnOl, the competing reinforcing effect of a crystalline dispersed phase of ZnOl overcomes the initial plasticization of the soluble portion and the modulus increases.

The tensile data for the compounds are summarized in Table 1. The Zn-SEPDM did not exhibit a yield stress, but the compounds did. The yield stress increased with increasing ZnOl, though the yield strain decreased (see Table 1). The tensile data above the yield stress of the compounds were not reliable due to the limited number of specimens tested and the difficulty in eliminating defects in the compression-molded samples.

Shape Memory Behavior. *Shape Fixing.* The shape fixing characteristics of the Zn-SEPDM/ZnOl compounds are shown in Figure 10. The ordinate of the graph corresponds to the fixing effectiveness, F, as defined by eq 1, following a deformation of the SMP at 100 °C (note that $T_{act} \sim 70$ °C) and fixing the temporary shape by quenching the sample in ice water and then removing the applied stress. After removal of the stress, the Zn-SEPDM/ZnOl compounds exhibited considerable relaxation of the temporary shape. First, there was an instantaneous recovery of the strain of ~10% when the stress was removed (see data at $t = 0$ in the inset of Figure 10) that was followed by a fast relaxation of the strain within the first hour and then a slow relaxation until a constant strain was achieved after about 300 h at room temperature. The extent of the creep recovery in the first hour was

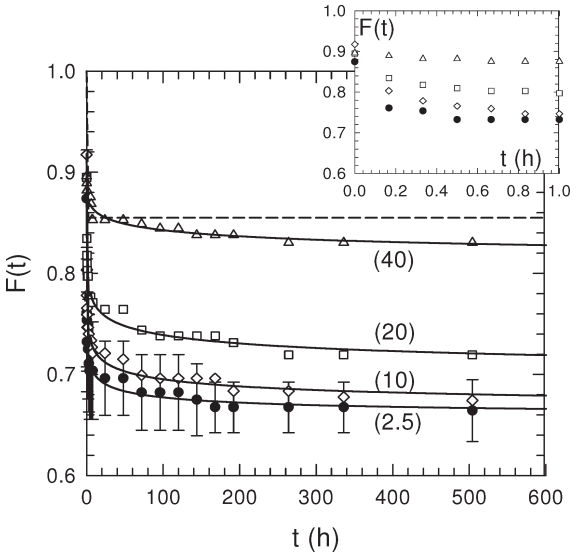

Figure 10. Shape fixing effectiveness at room temperature as a function of time for Zn-EPDM/ZnOl compounds following removal of stress after stretching a film to about 200% at 100 °C and then quenching the sample in ice water. Note that $T_c \sim 70$ °C. For clarity, error bars are shown only for one sample. The size of the error bars for the other samples is comparable. The inset graph shows the data for $t \leq 1$ h. The dashed curve is the fit of a single Voigt model (i.e., one retardation time), eq 7, to the data for the Zn-EPDM(40) sample. The solid curves are fits of eq 8.

dependent on the concentration of ZnOl. The lower the concentration, the higher was the creep recovery.

The points in Figure 10 represent the average of measurements of three separate specimens for each sample, and the error bars are the standard deviation.. For clarity, error bars are shown only for the data of the 2.5% ZnOl compound, but the standard deviation in the data for all of shape memory compounds was comparable. The equilibrium value of $F(t)$, F_{eq}, increased as the concentration of ZnOl increased. The data for the Zn-SEPDM-(50) was anomalous, which may be due to some macrophase separation of the fatty acid salt at the higher ZnOl concentration.

The data in Figure 10 essentially represent a creep recovery experiment—that is, the stretching step prior to fixing the temporary shape may be considered a step strain. For an ideal shape memory polymer, no strain recovery should occur ($F = 1$). However, the physical nature of the temporary network, as well as the permanent network in this work, leads to nonideal behavior. By defining time equal zero as the time when the stress is removed during the fixation step, the fixing effectiveness can be expressed in terms of strain by eq 5

$$F(t) = \frac{1}{1 + \varepsilon(0)}[1 + \varepsilon_R(t)] \quad (5)$$

where $\varepsilon(0) = (L_s - L_i)/(L_i)$ and $\varepsilon_R(t) = (L_f(t) - L_i)/(L_i)$; L_i is the original length of the molded specimen, and L_s and L_f are the stretched length prior to removing the stress during the fixation step and the length of the sample after removing the stress, respectively. The Voigt model, which is commonly used to calculate creep recovery of a viscoelastic fluid, is given by eq 6[20]

$$\varepsilon_R(t) = \varepsilon(0)e^{-t/\tau} \quad (6)$$

where τ is a retardation time. When this is substituted into eq 5, the fixing effectiveness becomes

$$F(t) = \frac{1}{1 + \varepsilon(0)}[1 + \varepsilon(0)e^{-t/\tau}] \quad (7)$$

The fit of eq 7 to the data for Zn-SEPDM(40) is shown by the dashed curve in Figure 10, and it is obvious from the poor fit that a single relaxation time is insufficient for describing the strain recovery data for these compounds. That is not unusual for a variety of reasons, most significant of which is that the network in these systems is likely to be inhomogeneous (e.g., a distribution of network chain lengths, entanglements, and cross-link density), the permanent cross-links and the temporary cross-links involve aggregated molecules with sizes ranging from nanometers for the microphase separation in the ionomer network[11] and hundreds of nanometers for the ZnOl crystals[11] that produce the temporary network, and both the permanent and temporary networks involve physical cross-links.

Gurlovenko and Gotlib[21] proposed that for an inhomogeneous cross-linked polymer a random arrangement of cross-links produces "percolation clusters" due to variations in cross-link density. They modeled the stress relaxation behavior of such networks using a stretched exponential function.[22] Baeurle et al.[23] used that model to predict the stress relaxation behavior of a homogeneously cross-linked network with transient cross-links. Specifically, they modeled the dynamics of block copolymers that form microphase-separated domains. The transient nature of the cross-links involved a mechanism by which stress pulls blocks of one polymer from a thermodynamically favorable domain into a thermodynamically unfavorable region of the other polymer.

The shape memory compounds used in the current study have a more complicated morphology than the block copolymers used by Gurlvenko and Gotlib.[23] These materials have three distinct chemical regions: (1) a continuous EPDM phase, (2) microphase-separated ionic domains (~1 nm)[11] that are covalently bonded to the EPDM, and (3) the dispersed ZnOl crystalline phase (~500 nm)[11] that is physically bonded to the sulfonate groups in the ionic phase. Nevertheless, the modeling strategies described in refs 21 and 23 to develop a stretched exponential equation for the strain recovery data in Figure 10

$$F(t) = F_{eq} + ce^{-(t/\tau)^{\beta}} \quad (8)$$

where $F_{eq} = F(\infty)$ = the equilibrium value for the fixing efficiency, $c = F(0) - F(\infty)$, τ is a characteristic retardation time, and β is the stretched exponential coefficient ($0 < \beta < 1$).

The retardation time, τ, is proportional to the maximum retardation time, and β is a function of the distribution of relaxation times.[21] However, β includes contributions from internal retardation of the domains as well as the retardation of the network,[23] which have not been resolved for this work. The parameters $F(0)$, F_{eq}, τ, and β for the fits of eq 8 shown by the solid curves in Figure 10 are listed in Table 2. The stretched exponential model fit the data in Figure 7 very well, and the $F(0)$ and F_{eq} parameters agree well with the results shown in Figure 10. There is some scatter in the ZnOl concentration dependence of the characteristic retardation time, but in general, τ increased with increasing ZnOl concentration. This result may be a consequence of the increased volume of the dispersed ZnOl phase and, thus, greater interfacial area for contact between the ZnOl phase and the ionic groups of the ionomer. It also may be related, in part, to the increased crystallinity of the ZnOl phase (see Figure 3). The value of τ was extremely high for the Zn-SEPEM(50), but as indicated earlier in this paper, there are some anomalies with the data for that sample. Although eq 8 fit the data, for that particular sample, the standard error of the parameters listed in Table 2 were actually larger than the values themselves. Though the meaning of β in Table 2 is not clear, since it involves two mechanisms that were not isolated in this study, it is worth noting that the values, at least up to 20 wt % ZnOl, were similar to those reported by Baeurle et al.[23] for a poly(styrene-*b*-isoprene-*b*-styrene) triblock copolymers (0.19 and 0.23 for two different styrene contents).

Table 2. Shape Fixing Efficiency and Shape Recovery Parameters[a]

[ZnOl], wt %	F_{eq}	$F(0)$	β	τ, h	r^2	R, %	std dev (R), %
2.5	0.658	0.875	0.171	0.599	0.986	103	6
5	0.700	0.917	0.237	0.383	0.989	119	28
10	0.622	0.878	0.158	1.08	0.981	84	7
20	0.676	0.876	0.188	11.8	0.979	92	9
30	0.763	0.903	0.385	1.21	0.931	79	13
40	0.815	0.897	0.297	75.8	0.946	73	1
50	0.605	0.850	0.087	3.0×10^6	0.924	123	22

[a] Average of three independent measurements; value in parentheses is the standard deviation.

The time dependency of the fixation of the temporary shape, as seen in Figure 10 and Table 2, is not desirable for a shape memory polymer. There are two potential sources of the time dependency in these compounds: 1) relaxation of the physical cross-links due to ionic group associations in the ionomer that provide the "permanent" network and 2) relaxation of the physical cross-links due to dipolar interactions between the metal sulfonate groups in the ionomer and the metal carboxylate groups of the ZnOl domains that form the temporary network. Previous work has shown that the physical cross-links in Zn-SEPDM ionomers are quite robust and produce an effective thermoplastic elastomer,[9] so one might expect the fixation problem for these compounds arises from creep in the temporary network. However, resolution of the source of the creep is not possible from the data presented in this paper. For these materials to provide useful shape memory properties, one needs to suppress the creep relaxation behavior shown in Figure 10. Current research on these materials is directed at isolating the source of the creep and assessing whether it can be eliminated sufficiently that useful shape memory behavior may be achieved.

Shape Recovery. The shape recovery effectiveness of the compounds following shape fixing with and without allowing time for the fixed shape to relax (see experimental details), calculated using eq 2, is plotted as a function of the ZnOl concentration in Figure 11. The differences in the results for the two procedures used, i.e., (1) recovery immediately following fixing the temporary shape and (2) recovery after aging the temporary shape for 21 days, are due to the creep relaxation of the temporary shape that occurred in the second procedure.

For the experiment in which recovery is measured immediately following the fixing of the temporary network (filled symbols in Figure 11), a maximum for the recovery effectiveness, ~90%, occurred for ZnOl concentrations of ~20−30 wt %. The poorer recovery effectiveness for compounds with ZnOl concentrations less than 20 wt % may be due to insufficient volume fraction of the ZnOl domains and too little interfacial area between the ZnOl domains and the ionomer so that some plastic deformation of the compound occurred during the initial stretching of

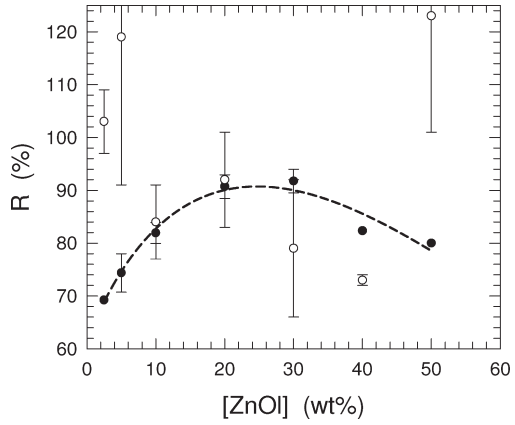

Figure 11. Shape recovery effectiveness for ZnOl/Zn-SEPDM compounds following stretching at 100 °C and fixing the temporary shape at 0 °C: (●) recovery at 100 °C immediately after fixing temporary shape; (○) after aging temporary shape at room temperature without stress for 21 days.

the compound. The poorer recovery efficiency at the higher concentrations, [ZnOl] > 30 wt %, may be a consequence of the plasticization of the ionic dipolar interactions by molten ZnOl, which provided the permanent cross-links, when the compound was heated above T_{act}, as was discussed earlier in this paper. In either case, it appears that changes in the SMP morphology and/or microstructure is the key for understanding the source(s) of the nonreversible deformation of these compounds. Current research is considering how or if morphological changes occur in these systems under loading and at elevated temperatures.

With the exception of the 50 wt % ZnOl compound, the recovery effectiveness for the samples aged in the temporary shape, but without stress, for 21 days, decreased with increasing ZnOl concentration. Some of these samples exhibited recovery efficiencies greater than 100%, which is a direct consequence of the strain recovery that occurred during the aging experiment and the definition of R (see eq 2). A strain recovery greater than 100% also suggests that a structural change of the network occurred, which again could be due to slippage or rearrangement of the permanent and/or temporary physical networks. For example, stress could pull the ionic part of the chain out of the microphase-separated ionic domains, which would change the equilibrium shape of the fully relaxed network. As a result, the final shape could be shorter than the length of the original sample, which would produce an R > 100%. For a shape memory material, however, a result of R > 100% is just as undesirable as R < 100%.

■ CONCLUSIONS

Compounds of an ionomer with a fatty acid or fatty acid salt (FAS) represent a new strategy for designing shape memory polymers (SMPs). Microphase separation of an ionic nanophase that arises from ionic interactions of the metal salt groups in the ionomer forms a physical cross-linked network with very long relaxation times. If the relaxation time is much longer than the characteristic time of the application, these physical interactions can essentially act as a permanent network. In contrast to other SM, where only polymer thermal transitions are used to form a reversible, temporary network, the temporary network in the ionomer/FAS compounds is derived from dipolar interactions between complementary metal salts that exist in the ionomer and the dispersed crystalline phase of the low molecular weight FAS.

The ionomer/FAS compound can be molded into a permanent shape and then reshaped by applying stress above a critical temperature, which corresponds to the melting point of the FAS, T_m. The temporary shape can be fixed by cooling the reshaped sample below T_m, and the original (permanent) shape can be recovered by reheating above T_m in the absence of a deforming stress. A weakness in the shape memory behavior of these compounds, however, is that the temporary shape exhibits significant time-dependent relaxation. A ∼10% retraction of the shape occurred immediately upon removal of the stress, independent of the ZnOl concentration. This was followed by a stretched exponential decrease of the sample length. As the ZnOl concentration increased from 2.5 to 40 wt %, the creep retardation time increased by 2 orders of magnitude and the equilibrium length of the sample increased from 66% to 82% of the temporary shape length. Despite the relaxation of the temporary length, shape recovery of the compounds was as high as 90%.

The suppression of the creep recovery behavior with increasing ZnOl concentration is due to an increase in the interfacial area between the ionomer and the dispersed FAS phase, which would be expected to retard the relaxation of the temporary shape. The increase in the ZnOl concentration also increased the modulus of the compounds. The origin of the relaxation of the temporary shape is creep of the temporary network (ionomer−ZnOl) and/or creep of the permanent network (ionic domains in the ionomer). In the latter case, the residual stress in the network chains may be sufficient to pull ionic groups out of one domain and allow them to "hop" to another domain, thus changing the microstructure of the permanent network. Alternatively, stress could disrupt the dipolar interactions between the metal sulfonate groups of the ionomer and the metal carboxylate groups of the ZnOl crystalline domains, allowing movement of the temporary network.

Although one might expect the weaker dipolar interactions that comprise the temporary network to be the culprit in the time dependency of the temporary shape, creep of the ionic network within the ionomer cannot be ruled out as part or even most of the source of the deficiency of the shape memory behavior. Current research is being directed at identifying which mechanism is responsible. The Zn-SEPDM contains unsaturation that can be used to covalently cross-link the polymer via free-radical chemistry, e.g., by electron beam radiation. In that case, the permanent network should not exhibit time-dependent behavior and the dynamics of the temporary network can be isolated. Note that the ionomer is a necessary component in this design of a SMP even if the ionic microphase separation is not used for the permanent cross-link. Without the ionic groups, the FAS will not mix with the elastomer (in this case, EPDM). However, with the inclusion of as low a metal sulfonate concentration of ∼1 sulfonate per 150 repeat units (as in this study), the compatibility of ZnOl increases from <1 wt % to as high as 50 wt %.

Although the ionomer/FAS compounds described in this paper may have application as SMPs, the time-dependent behavior described in this paper must be eliminated. This first requires an improved understanding of the dynamics of these materials as well as changes in the microstructure that may be produced.

■ AUTHOR INFORMATION

Corresponding Author

*E-mail: rweiss@uakron.edu.

■ ACKNOWLEDGMENT

This research was supported by a grant from the Polymer Division of the National Science Foundation (DMR-0960461).

■ REFERENCES

(1) Mather, P. T.; Luo, X.; Rousseau, I. A. *Annu. Rev. Mater. Res.* **2009**, *39*, 445–471.
(2) Liu, C.; Qin, H.; Mather, P. T. *J. Mater. Chem.* **2007**, *17*, 1543–1558.
(3) Lendlein, A.; Kelch, S. *Augew. Chem., Int. Ed.* **2002**, *41*, 2034–2057.
(4) Ratna, D..; Karger-Kocsis, J. *J. Mater. Chem.* **2008**, *43*, 254–269.
(5) Huang, W. M.; Yang, B.; Zhao, Y.; Ding, Z. *J. Mater. Chem.* **2010**, *20*, 3367–3381.
(6) Rousseau, I. A. *J. Mater. Chem.* **2008**, *48*, 2075–2089.
(7) Xie, T.; Page, K. A.; Eastman, S. A. *Adv. Funct. Mater.* **2011**, *21*, 2057.
(8) Weiss, R. A.; Izzo, E.; Mandelbaum, S. *Macromolecules* **2008**, *41*, 2978–2980.
(9) Makowski, H. S.; Lundberg, R. D.; Westerman, L.; Bock, J. In *Ions in Polymers*; Eisenberg, A., Ed.; American Chemical Society: Washington, DC, 1980; pp 3−20.
(10) Behl, M.; Lendlein, A. *Mater. Today.* **2007**, *10*, 20–28.
(11) Jackson, D. A.; Koberstein, J. T.; Weiss, R. A. *J. Polym. Sci., Phys. Ed.* **1999**, *37*, 3141–3150.
(12) Chung, T.; Romo-Uribe, A.; Mather, P. T. *Macromolecues* **2008**, *41*, 184–192.
(13) Zotzmann, J.; Behl, M.; Hofmann, D.; Lendlein, A. *Adv. Mater.* **2010**, *22*, 3424–3429.
(14) Wakabayashi, K.; Register, R. A. *Ind. Eng. Chem. Res.* **2010**, *49*, 11906–11913.
(15) Zhang, L.; He, R.; Gu., H.-C. *Appl. Surf. Sci.* **2006**, *253*, 2611–2617.
(16) Sahoo, Y.; Pizem, H.; Fried, T.; Golodnitsky, D.; Burstein, L.; Sukenik, C. N.; Markovich, G. *Langmuir* **2001**, *17*, 7907–7911.
(17) Barman, S.; Vasudevan, S. *J. Phys. Chem. B* **2006**, *110*, 651–654.
(18) Sato, Y.; Furukawa, J. *Rubber Chem. Technol.* **1963**, *36*, 1081–1160.
(19) Makowski, H. S.; Lundberg, R. D. In *Ions in Polymers*; Eisenberg, A., Ed.; American Chemical Society: Washington, DC, 1980; pp 37−51.
(20) Ferry, J. D. *Viscoelastic Properties of Polymers*, 3rd ed.; Wiley: New York, 1980.
(21) Gurtovenko, A. A.; Gotlib, Y. Y. *J. Chem. Phys.* **2001**, *115*, 6785–6793.
(22) Williams, G.; Watts, D. C. *Trans. Faraday Soc.* **1970**, *66*, 80–85.
(23) Baeurle, S. A.; Hotta, A.; Gusev, A. A. *Polymer* **2005**, *46*, 4344–4354.